Electronic Supplementary Material (ESI) for Nanoscale

Evidencing a mask effect of graphene oxide: a comparative study on primary human and murine phagocytic cells

Julie Russier,[a]*, Emanuele Treossi,[b] Alessia Scarsi,[c] Francesco Perrozzi,[d] Hélène Dumortier,[a] Luca Ottaviano,[d] Moreno Meneghetti,[c] Vincenzo Palermo[b] and Alberto Bianco*[a]

[a]CNRS, Institut de Biologie Moléculaire et Cellulaire, Immunopathologie et Chimie Thérapeutique/Laboratory of Excellence Medalis, Strasbourg, France.
[b]CNR-ISOF, Bologna, Italy
[c]Dipartimento di Scienze Chimiche, Università di Padova, Padova, Italy
[d]Dipartimento di Fisica, Università dell'Aquila, L'Aquila, Italy

Electronic Supplementary Information

A		Controls		100 µg/ml			50 µg/ml			25 µg/ml			10 µg/ml			1 µg/ml		
		Control	DMSO/ H_2O_2/PMA LPS+IFNγ/LPS	0h-GO	2h-GO	26h-GO	0h-GO	2h-GO	26h-GO	0h-GO	2h-GO	26h-GO	0h-GO	2h-GO	26h-GO	0h-GO	2h-GO	26h-GO
Cellular viability (% of total)		62.7 12.7	26.9 8.9	19.6 7.7	19.4 9.0	15.0 6.7	35.4 11.9	29.6 12.2	22.2 9.3	46.2 11.7	38.7 12.3	44.0 10.6	52.5 12.7	55.8 12.8	57.3 10.6	59.4 13.3	63.6 13.3	63.2 12.8
ROS generation (% of control)		100	99.5 2.4	103.0 17.7	129.0 29.6	111.0 13.5	98.3 18.3	128.7 23.1	141.2 20.2	91.4 10.5	143.3 36.0	137.7 23.9	89.6 11.5	146.7 39.9	139.9 31.5	93.1 7.6	104.6 15.5	100.1 16.7
CD86 expression (% of control)		100	37.7 15.3	157.3 23.9	182.2 34.1	187.4 34.4	150.5 22.6	151.9 22.0	158.5 24.5	123.5 13.4	136.9 16.9	129.3 14.2	104.6 14.0	127.9 10.5	116.4 10.8	98.7 6.8	108.4 3.0	108.2 3.9
Cytokine production (pg/ml)	TNFα	N.D.	823.9 251.9	2.3 2.451	7.4 3.1	0.3 2.2	12.8 6.9	16.3 6.9	15.1 6.7	6.7 4.6	4.3 4.9	7.5 6.5	0.4 2.9	N.D.	3.7 6.0	N.D.	N.D.	N.D.
	IL1β	N.D.	34.6 7.7	7.7 8.3	N.D.	N.D.	2.9 3.2	N.D.	N.D.	2.9 3.2	N.D.	N.D.	N.D.	N.D.	N.D.	N.D.	N.D.	N.D.
	IL6	67.8 60.0	3492.2 407.1	9.1 7.2	N.D.	N.D.	16.4 13.5	12.94 12.7	14.1 14.9	44.8 25.0	36.4 25.8	52.2 48.4	25.3 18.7	25.8 21.0	67.6 56.9	46.8 40.0	42.3 34.9	65.7 42.6

B		Controls		100 µg/ml			50 µg/ml			25 µg/ml			10 µg/ml			1 µg/ml		
		Control	DMSO/ H_2O_2/PMA LPS+IFNγ/LPS	0h-GO	2h-GO	26h-GO	0h-GO	2h-GO	26h-GO	0h-GO	2h-GO	26h-GO	0h-GO	2h-GO	26h-GO	0h-GO	2h-GO	26h-GO
Cellular viability (% of total)		66.3 4.8	3.0 1.1	31.5 12.2	22.2 11.2	28.2 12.6	38.3 12.7	28.6 11.4	25.1 9.5	34.8 10.9	26.9 11.4	28.0 12.8	35.6 11.0	30.3 9.5	30.7 10.7	39.4 5.1	54.8 3.3	51.4 4.3
ROS generation (% of control)		100	117.0 4.9	137.4 33.8	286.8 82.7	198.5 67.3	122.0 24.5	324.6 84.0	280.4 86.5	114.2 25.0	375.6 77.6	311.3 82.0	118.0 19.4	421.0 79.4	392.1 78.4	113.5 6.0	223.1 18.8	272.9 58.8
CD86 expression (% of control)		100	115.8 11.7	96.6 25.5	203.3 40.6	212.8 39.0	78.0 22.3	155.9 16.6	172.8 4.2	74.9 20.3	115.8 3.1	157.6 16.4	64.0 15.3	95.9 14.9	113.2 21.9	64.0 9.5	108.2 12.1	110.0 10.2
Cytokine production (ng/ml)	TNFα	0.4 0.1	4.1 0.8	1.9 0.5	5.6 1.3	7.2 1.8	2.0 0.4	5.2 1.398	6.4 1.7	1.5 0.3	2.9 0.9	3.8 1.2	1.1 0.2	1.3 0.3	2.3 0.8	0.7 0.1	0.5 0.1	0.5 0.1
	IL1β	0.2 0.1	1.2 0.3	0.8 0.3	0.5 0.2	0.8 0.3	1.1 0.3	0.9 0.3	1.3 0.5	1.1 0.2	0.7 0.2	1.2 0.4	0.9 0.2	0.5 0.1	0.7 0.2	0.5 0.2	0.2 0.1	0.2 0.1
	IL6	8.0 1.7	58.9 13.7	3.4 1.2	1.7 0.9	3.2 1.1	6.3 1.9	3.1 1.1	5.0 1.288	7.8 1.8	3.9 1.2	5.0 1.1	8.6 2.0	4.5 2.0	5.1 1.3	7.8 1.7	7.4 1.6	7.2 1.4

Table S1. Summary of the different parameters taken into account in the evaluation of our 0h-GO, 2h-GO and 26h-GO impact on human monocyte derived macrophages, hMDM (A) and primary murine intraperitoneal macrophages, mIPM (B). Mean values of at least 3 independent experiments are showed ± SEM.

Target	Capture Antibody	Detection Antibody	Cytokine Recombinant
Human TNFα	*Purified Anti-Human TNFα* BD Biosciences 51-26371E (from ELISA Set 555212)	*Biotinylated Anti-Human TNFα* BD Biosciences 51-26372E (from ELISA Set 555212)	*Recombinant Human TNFα* BD Biosciences 51-26376E (from ELISA Set 555212)
Human IL1β	*Purified Anti-Human IL1β* BD Biosciences 51-9002512 (from ELISA Set 557953)	*Biotinylated Anti-Human IL1β* BD Biosciences 51-9002516 (from ELISA Set 557953)	*Recombinant Human IL1β* BD Biosciences 51-9004477 (from ELISA Set 557953)
Human IL6	*Purified Anti-Human IL6* BD Biosciences 51-26451E (from ELISA Set 555220)	*Biotinylated Anti-Human IL6* BD Biosciences 51-26452E (from ELISA Set 555220)	*Recombinant Human IL6* BD Biosciences 51-26456E (from ELISA Set 555220)
Murine TNFα	*Purified Hamster Anti-Mouse/Rat TNFα* BD Pharmingen 557516	*Biotin Rabbit Anti-Rat/Mouse TNFα* BD Pharmingen 557432	*Recombinant Mouse TNFα* BD Pharmingen 554589
Murine IL1β	*Purified Anti-Mouse IL1β* BD Biosciences 51-26661E (from ELISA Set 559603)	*Biotinylated Anti-Mouse IL1β* BD Biosciences 51-26662E (from ELISA Set 559603)	*Recombinant Mouse IL1β* BD Biosciences 51-26666E (from ELISA Set 559603)
Murine IL6	*Purified Rat Anti-Mouse IL6* BD Pharmingen 554400	*Biotin Rat Anti-Mouse TNFα* BD Pharmingen 554402	*Recombinant Mouse IL6* BD Pharmingen 554582

Table S2. Specific capture and detection antibody pairs and recombinant proteins used for ELISA determination of human and murine TNFα, IL6 and IL1β concentration in the cellular culture supernatant.

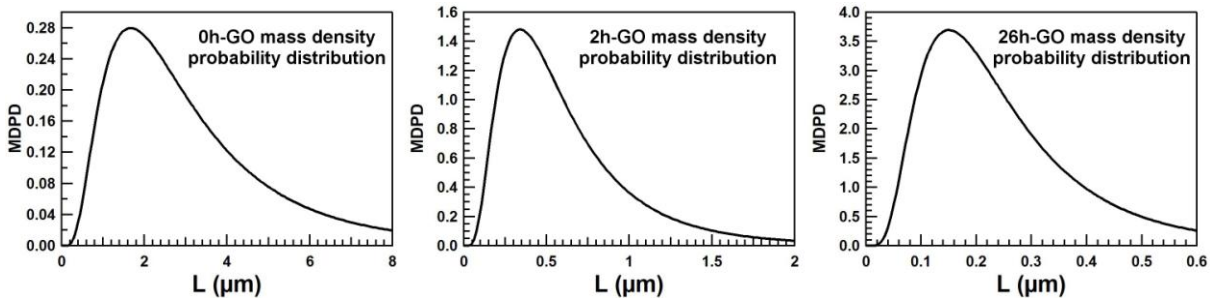

Figure S1. Mass density probability distribution of the large 0h-GO, small 2h-GO and very small 26h-GO samples.

The mass density probability distribution (MDPD) function can be written as:

$$MDPD = \frac{n(L)L^2}{M_{tot}}$$

$$M_{tot} = \int_0^{inf} L^2 n(L)\,dL$$

where L represent the lateral size of the single layer GO and $n(L)$ the lateral size distribution. By integrating the MDPD in a specific range, it is possible to determine the fraction of the concentration of single layer GO with those specific dimensions. In the case of 0h-GO solution for example, the single layer with a dimension higher than 1 μm represents ~92% of the concentration.

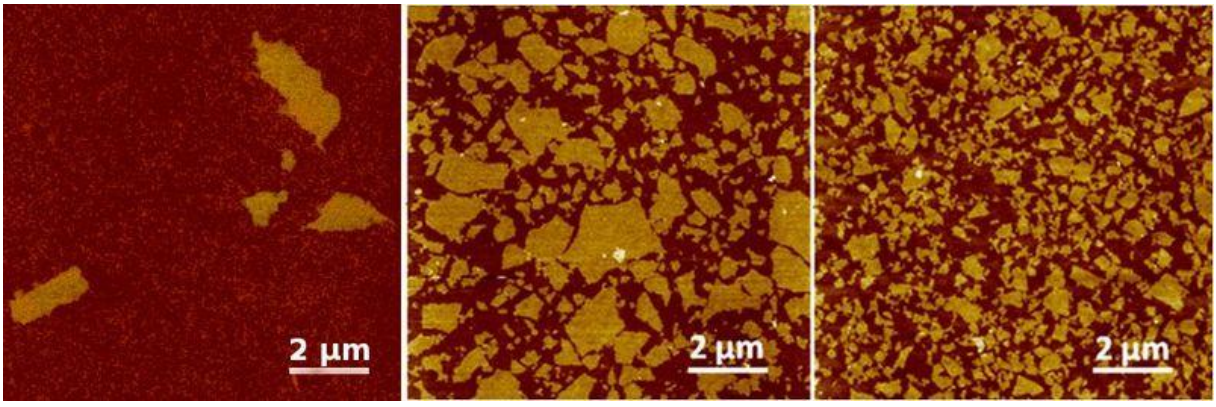

Figure S2. AFM images of GO single layers obtained by spin-coating of 0h-GO (a), 2h-GO (b) and 26h-GO (c) dispersions.

We would like to point out that an inconsistency between the results of the statistical analysis of the flake size distribution and a more straightforward (though misleading) rough analysis made by simple visual inspection of the SEM and AFM images can be observed. Indeed, a rough eye-guided estimation of the average flake size leads to a significant over-estimation of the average flake size (with respect to the correct one determined *via* the statistical analysis). This apparent inconsistency is essentially due to the inherent asymmetry and positive skewness of the log-normal distribution. Visual inspection leads to focus on counting very large flakes, which actually contribute with a proportionally low count rate in a more accurate statistical analysis. Moreover, it is worth stressing that, for a very accurate determination of the flakes size distribution, SEM analysis (see Figure 1) is much more effective and accurate than AFM as one can scan by far large sample areas.

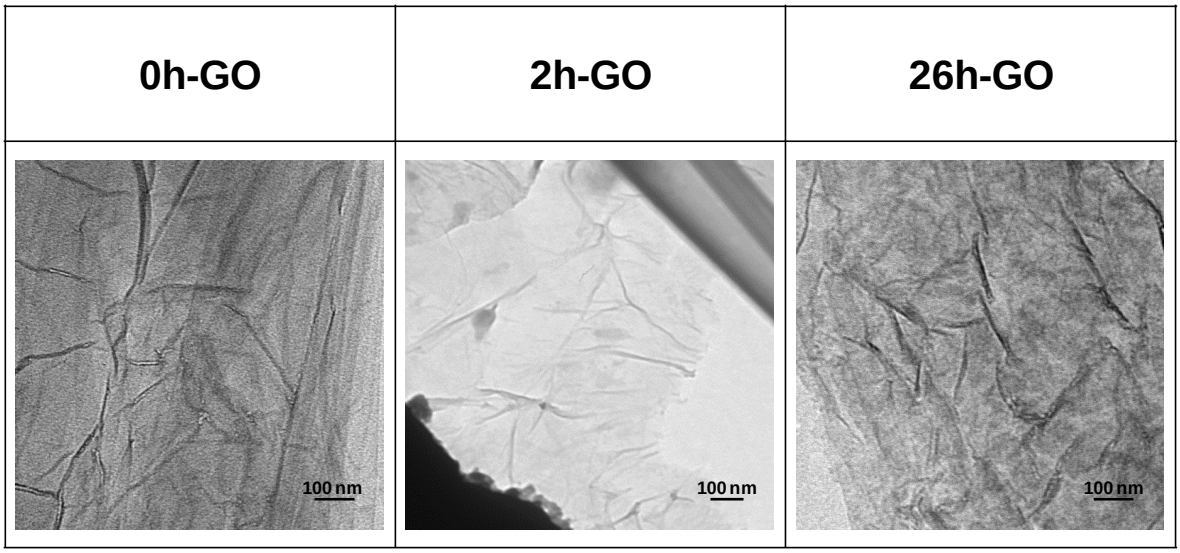

Figure S3. TEM images of GO sheets. Samples (50 µg/ml) were deposited on copper grids and allow drying prior to TEM observation.

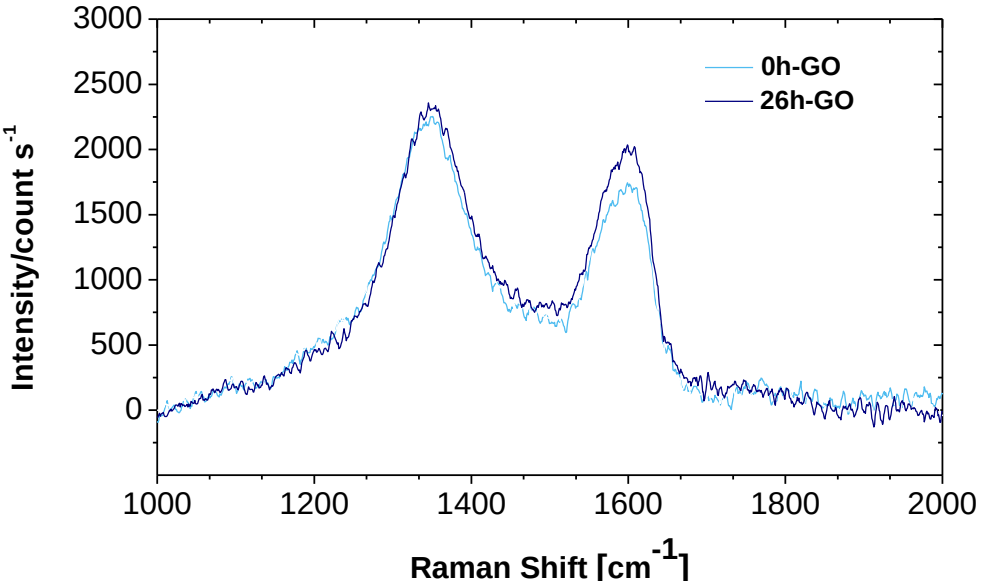

Figure S4. Raman spectra of a film obtained by drop casting on a glass slide of non sonicated (light blue), and sonicated for 26 hours (blue) GO.

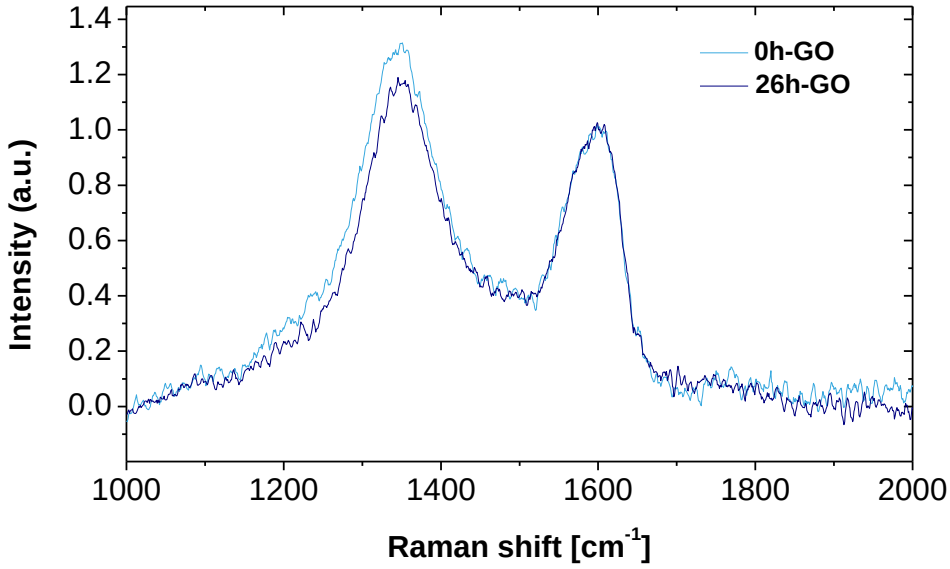

Figure S5. Raman spectra reported in Figure S4 normalized on the G band.

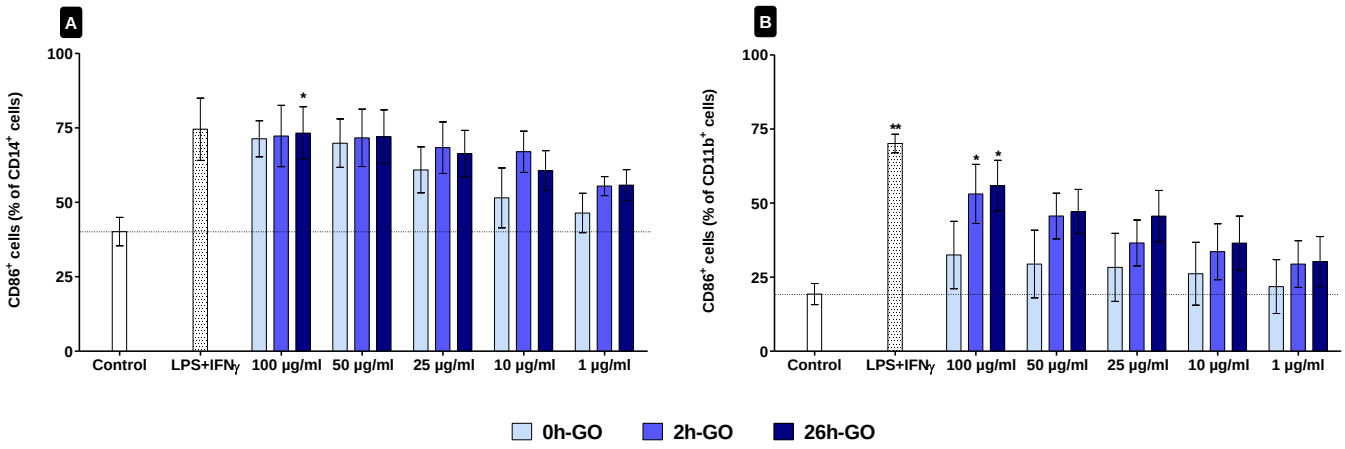

Figure S6. Flow cytometry analysis of the percentage of $CD86^+$ cells out of the $CD14^+$ hMDM (A) or $CD11b^+$ mIPM (B) populations after incubation with 0h-, 2h- and 26h-GO (1 to 100 µg/ml). Two-ways ANOVA followed by Bonferroni's post-test was performed to determine the statistical differences versus control cells and to compare the three GO samples to each other (*$p<0.05$; **$p<0.01$; ***$p<0.001$).

In hMDM, the percentage of $CD86^+$ cells was significantly affected only following the incubation with 26h-GO at the highest concentration (100 µg/ml). On the other hand, the incubation with 0h- and 2h-GO at all the tested concentrations or 26h-GO from 1 to 50 µg/ml did not determine any significant modification of this co-stimulatory molecule expression. Nevertheless, a slight concentration related augmentation of the $CD86^+$ cells could be observed, consistently with the geomean fluorescence intensity registered (GMFI; see Figure 6). Finally, the number of cells expressing CD86 seemed to be more important after incubation with the smaller size GO (2h- and 26h-GO) respect to the large GO sample (0h-GO). This GO lateral dimension associated trend was better evidenced in murine cells. In fact, consistently with the GMFI studies, the number of $CD86^+$ cells was significantly increased following incubation with small size GO at 100 µg/ml (2h- and 26h-GO) and 50 µg/ml (26h-GO). It is important to note that, even though the statistical significance was not reached using the other concentrations, the $CD86^+$ cells percentage always followed the tendency 26h-GO>2h-GO>>0h-GO. In other words, the smaller GO samples were, the more they induced CD86 expression in a concentration related manner.

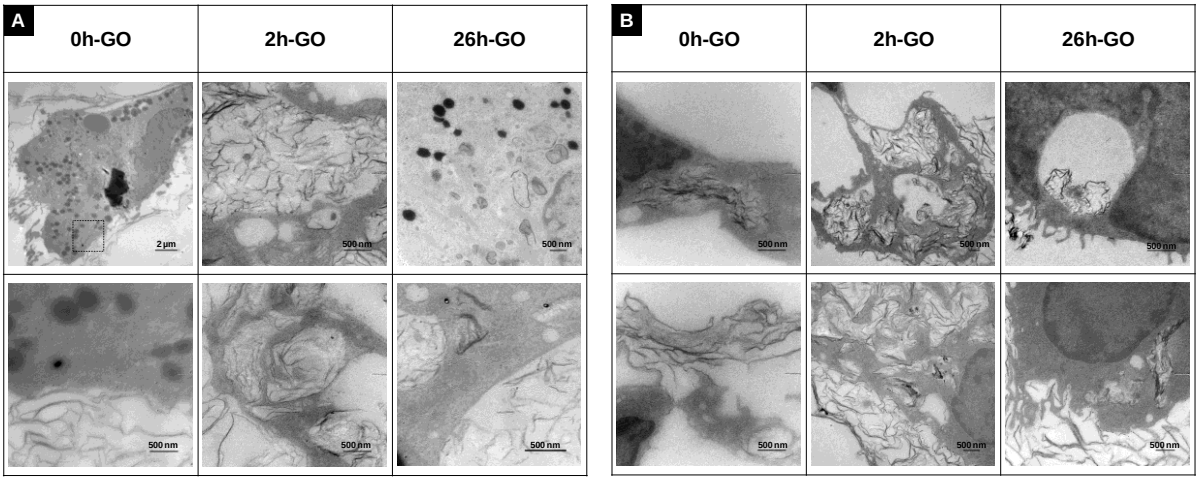

Figure S7. TEM images of hMDM (A) and mIPM (B) incubated with 0h-GO, 2h-GO and 26h-GO (50 µg/ml) during 24 h. When identified, the doted area in the top image is enlarged in the respective bottom picture. Details of the intracellular presence of GO samples (top row) and of their particular interaction with cellular membrane (bottom row) are shown.

TEM analysis of human and murine macrophages following the incubation with 0h-, 2h- and 26h-GO allowed identifying GO material inside both types of cells. As the precise mechanism underlying the cellular uptake of GO is still not fully understood, the fact that it was possible to observe GO sheets even in vescicles or free in the cytoplasm suggests that GO could be internalized by both active mechanisms (e.g. endocytosis) or passively pierce the cellular membrane. The further investigation of the interaction between GO and the cellular membrane highlighted how GO sheets dispose themselves parallel to the cellular surface. This particular disposition of the GO sheets is likely to allow their tight interaction with the cellular membrane, facilitating their passive internalization. Moreover, it could be seen, especially in mIPM, that several layers of GO sheets formed a sort of mask around the cells. This kind of cellular encasement not only supports the GO strong affinity for the cellular membrane but could also represent crucial factor in their subsequent effects on cellular parameters (i.e. cellular viability, ROS generation, activation).

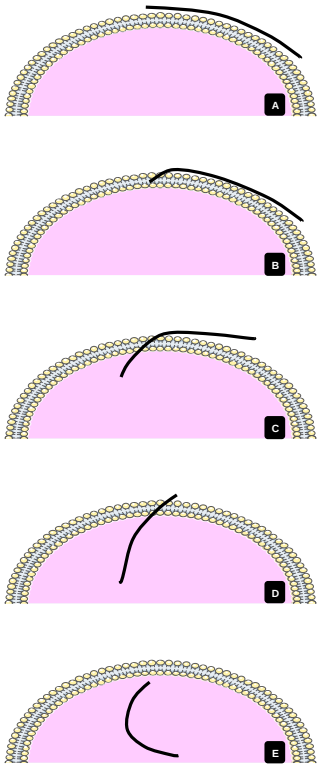

Figure S8. Hypothesized mechanism for GO passive internalization. First, the GO sheets dispose themselves parallel to the cellular membrane (A). Then, due to the tight interaction between GO and the cellular membrane, the edge of the GO flake pierces the phospholipid bilayer (B), begins to passively enter the cellular membrane (C and D) and finally reaches the intracellular compartment (E).